15th Australasian Fluid Mechanics Conference
The University of Sydney, Sydney, Australia
13-17 December 2004

A Directional Event Detector for Conditional Laser Imaging

P. V. Lanspeary[1] **and S. K. Lee**[1]

[1]School of Mechanical Engineering
The University of Adelaide, Adelaide, South Australia, 5005 AUSTRALIA

Abstract

Conditional sampling of laser-image data in bi-directional non-periodic unsteady flows requires an event detector which can resolve the characteristic direction of the flow. To avoid storing data which does not contain events of interest, event detection must be performed in real time. This paper describes a mixed analogue-TTL circuit which determines the characteristic flow direction from signals at three analogue inputs. When the analogue inputs indicate an event arriving from the preferred direction, the detector allows trigger signals to reach the imaging camera.

The event detector has been used for conditionally-sampled PIV of the internal flow in an oscillating-jet nozzle. In this particular example, streamlines of the conditionally-averaged flow have a spiral focus and two half saddles which are not resolved by conventional time averaging.

Introduction

Conditional sampling is a well-established method for investigating the structure of unsteady flows. Van Atta [9] provides an early history, and Antonia [1] describes a number of variations on the technique. Before the development of laser imaging for experimental research, conditional sampling was most often used in conjuction with hot-wire anemometry or cold-wire thermometry.

The essence of conditional averaging is to detect an event in the flow and to use the time or location of the event as an origin or reference point for ensemble averaging. The conditional-averaging process therefore has two components, (a) ensemble averaging, and (b) event-detection. For the measured parameter u, a simple form of ensemble average can be written as

$$\langle u(\mathbf{x},t)\rangle = \frac{1}{N}\sum_{i=1}^{N} u(\mathbf{x},\, t+\tau_i), \qquad (1)$$

where $\mathbf{x}$ is the space domain, t is the time domain, and events are detected at N points in time, $\{\tau_i : 1 \le i \le N\}$. The average may include a weighting function. For quasi-periodic flows such as oscillating jets, time between adjacent events may mapped onto the interval $[0, 2\pi]$ so that the conditionally-averaged parameter $\langle u(\mathbf{x},t)\rangle$ becomes periodic [11].

Event detection is less easy to summarise because the available choice of detection criterion is virtually unlimited, especially if the data is recorded continuously and the detection algorithm is applied to the recorded data. Some of the simpler schemes only compare the instantanteous event signal with a fixed discriminator level. Readers interested in a more detailed discussion of event-detection may wish to consult reviews and other articles on conditional sampling [1, 2, 6, 8, 9, 10].

In years before 1990, conditional sampling was used with hot-wire and other point-measurement sensors. The usual procedure was to store a continuous data record first; then a conditional-sampling filter would selectively extract data from the record and deliver it to the averaging algorithm. For PIV, the volume of data from the apparatus is so high that data not containing events of interest cannot be stored, and event detection must be performed in real time.

Of published investigations making use of conditionally-sampled PIV, the largest proportion ($\approx 53\%$) synchronise the PIV sampling with the phase of mechanically or acoustically driven unsteadiness in the flow (for example, Li et al. [5]). Another 37% are investigations of flow produced by turbines, rotary pumps or helicopter rotors where PIV is phase-locked to the rotation of a shaft.

At the time of writing, the authors know of only five examples (i.e. the remaining 10% of articles) of conditionally-sampled PIV where there was no apparent external excitation of the unsteady flow and the event-detection signal was obtained from the flow itself. Of these only one oscillating flow, the precessing-jet flow of Wong et al. [12] was bi-directional. Wong used an Atmel 8-bit microprocessor to resolve the direction of oscillation. In this paper, we present an alternative method of sensing direction — that is, with a TTL circuit.

Design Requirements

The specific requirement is for a device which controls the conditional sampling of PIV in a naturally oscillating-jet flow. The oscillating jet is produced by flow through an orifice into a short but larger diameter chamber (Figure 1). Flow from the inlet orifice reattaches asymmetrically and precesses around the circumference of the chamber [4]. For the tests described in this paper the event detector receives signals from an array of three pressure sensors which are distributed over part of the circumference and are turned to face the inlet orifice.

It is important not to bias the conditional average by using a detection algorithm which does not account for asymmetry of the unsteady flow. If, for example, precession in either direction were equally probable, a detection scheme which lacks sensitivity to direction would produce false symmetry in the conditional averages [3]. We therefore require that sampling occur only when precession is in a specified direction (i.e. clockwise or counter-clockwise). With three sensors, the event detector can also perform a crude form of spatial correlation so that small-scale features in the flow are less likely to be accepted as events.

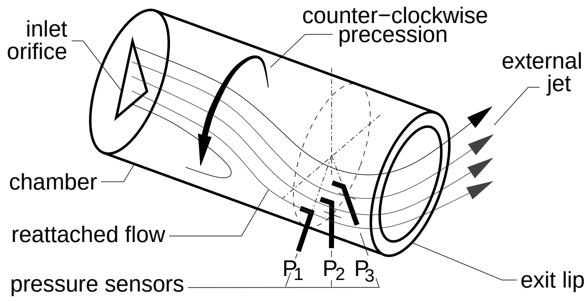

Figure 1: Schematic diagram of oscillating-jet device, with event-detecting pressure sensors.

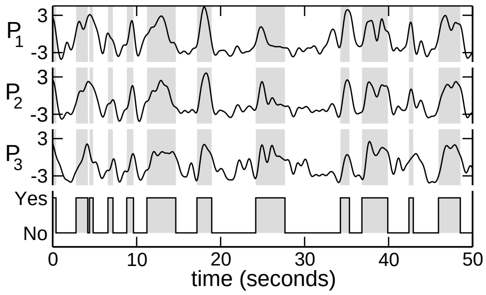

Figure 2: Comparison of pressure-sensor signals P_1, P_2, P_3 (Volts) and directly observed alignment of flow reattachment with the pressure sensors (Yes/No).

The pressure sensors produce a well defined signal peak when flow reattachment is aligned with the sensors (Figure 2) and so the initial step in event detection is to compare the signal with a suitable threshold level. To obtain the results shown in Figure 2, the alignment of flow reattachment is observed by using air bubbles as a flow-visualisation tracer. The working fluid is water.

The main operational requirement is that the event detector be installed as a switch in the camera-trigger line. The state of the switch is determined by the analogue signals from the pressure sensors. Figure 3 shows a typical arrangement of equipment for PIV. Recording the analogue signals and the conditioned camera trigger (via an A/D converter) is strongly recommended.

Description of Event Detector

The functional blocks of the event detector are a “threshold source”, a “comparator” for each analogue-signal input, and a “direction-detector logic” block (Figure 4). The circuit elements which, under control of the detection logic, enable and disable the camera trigger are little more than an “AND” logic gate.

The text which follows only describes how the most important parts of the circuit work. Many standard details and refinements familiar to technicians are omitted.

Adjustable threshold source

The circuit shown in Figure 5 produces rising-edge and falling-edge threshold voltages for the comparators. The comparator output is low when the pressure signal is below the falling-edge threshold, and is high when the pressure signal is above the rising-edge threshold. For stability of the comparator output, the rising-edge threshold must always be higher than the falling-edge threshold.

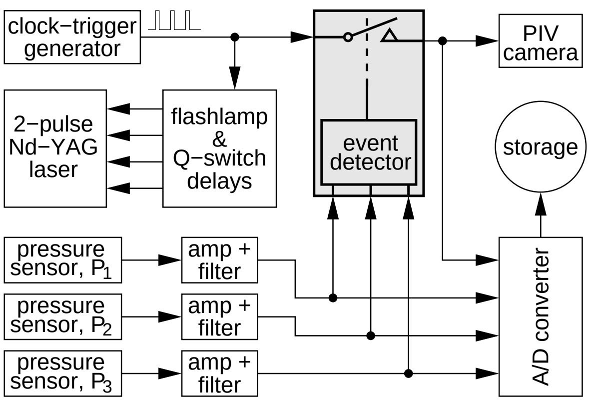

Figure 3: Installation of event detector for conditionally sampled PIV.

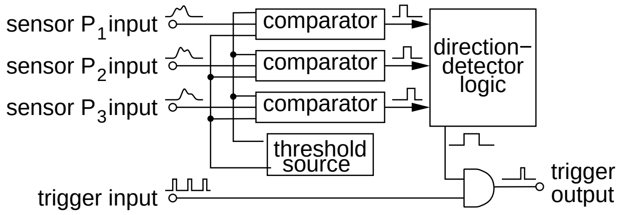

Figure 4: Event-detector functional blocks.

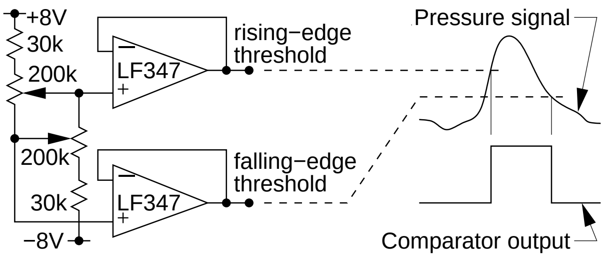

Figure 5: Adjustable threshold-source circuit.

Comparator

The main elements of the comparator circuit are shown in Figure 6. The output of the circuit is connected to the control input of a two-way (CMOS 4053) multiplexer so that a low output selects the rising-edge threshold and a high output selects the falling-edge threshold.

Instability or oscillation is a common problem with analogue comparators because of their high gain and bandwidth [7]. Both the LF347 and “positive feedback network” in the circuit diagram are intended to reduce instability. Details of the “positive feedback network” are given in Figure 1 of the National Semiconductor datasheet [7]. The network provides sufficient hysteresis for sharp output transition with signals of only a few Hertz. Small oscillations, which appear at slew rates lower than 100 mV/s, are cleaned up by adding a 40106 Schmitt trigger. The second Schmitt trigger serves only as an inverter.

Direction-detector logic

Figure 7 is a TTL circuit for detecting the counter-clockwise precession portrayed in Figure 1. Timing sequences for counter-

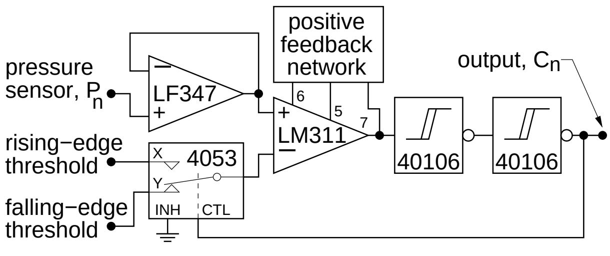

Figure 6: Comparator circuit (one of three); “LF347” is an op-amp, “4053” is a two-way multiplexer (i.e. switch), “LM311” is a comparator, “40106” is an inverting Schmitt trigger.

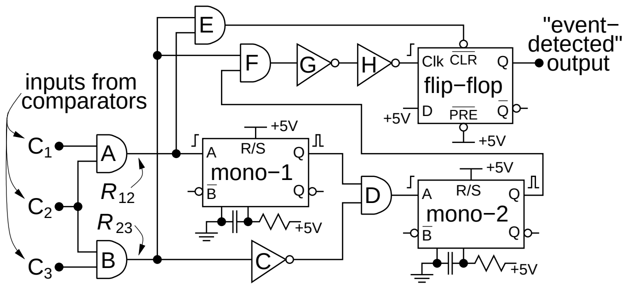

Figure 7: Direction-detector circuit; "mono" is a monostable multivibrator; "flip-flop" is a 7474 D-type flip flop; A, B, D, E and F are "AND" gates; C, G and H are inverters.

clockwise and clockwise precession are shown in Figure 8. Via the comparators, there are inputs from the three pressure sensors. Logic gates A and B combine signals from adjacent pressure sensors so that the distance between sensors determines the minimum physical size of flow feature which is likely to be detected. The outputs of gates A and B are

$$R_{12} = C_1 \text{ and } C_2, \tag{2}$$

$$R_{23} = C_2 \text{ and } C_3 \tag{3}$$

respectively. When R_{12} rises to a logic TRUE state, the first monostable (mono-1) produces a pulse which has a width of only a few microseconds. If the pulse passes through gate D, it "tells" the second monostable (mono-2) that an event has arrived at sensors P_1 and P_2, but has not arrived at sensors P_2 and P_3. Mono-2 then generates a pulse which, for a "detection lag" time equal to the pulse width, allows a rising edge at R_{23} to set the "event detected" output of the flip flop. If R_{23} does not produce a rising edge within the duration of the pulse from mono-2, an event is not detected. Inverters G and H provide the necessary "settling-time" delay from the $\overline{\text{CLR}}$ input to the Clk input of the flip flop. In summary, an event begins when R_{23} becomes TRUE, but only if this transition occurs within a specified "detection lag" time of a rise in R_{12}. When either of R_{12} or R_{23} become FALSE, the flip-flop is cleared and the event ends.

If precession is clockwise, R_{23} rises while R_{12} is already TRUE, the pulse from mono-1 is suppressed by gate "D", and an event is not detected. In this case, mono-1 prevents mono-2 from being triggered at the *trailing* edge of R_{23}.

Experimental Test Results

Conditionally-sampled PIV measurements were made of the flow inside an oscillating-jet device of the type shown in Figure 1. The working fluid was water seeded with 20 μm-diameter polyamid spheres. The Reynolds number based on flow at the inlet orifice was 70,000. Pulsed illumination of the seed particles was from a laser-light sheet normal to the axis of the chamber, and so only the non-axial components of velocity (V, W) were measured. The location of the laser-light sheet, pressure sensors and PIV camera are given in Figure 9. The area expansion ratio from the inlet orifice to the chamber is 3.5^2.

Seven hundred and twenty PIV-image pairs were obtained by unconditional sampling at the laser-pulse rate of 10 Hz. Another data set of the same size was obtained by conditional sampling with the event detector. Velocity vectors were calculated by cross-correlation with 32×32-pixel interrogation windows having 50% overlap. The mean and r.m.s. velocity magnitudes, and the mean streamlines of each data set are plotted in Figure 10. It is important to note that the much larger axial velocity component (U) is not measured by the PIV. The confidence intervals

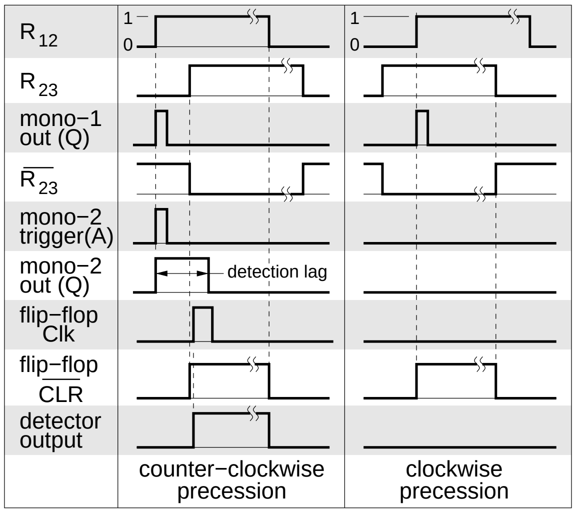

Figure 8: Schematic waveforms of the direction-detector signals for counter-clockwise and clockwise precession.

for the mean velocity magnitudes vary from ± 0.012 to ± 0.015. Most of the non-axisymmetry in Figure 10(a–c) may therefore be due to insufficient data, and most of the variation in the magnitude of the mean flow (Figure 10(a)) is likely to be statistical scatter.

The mean-flow streamlines in Figure 10(b) show that the only detail preserved by the non-conditional averaging is a star node. Flow streamlines for the conditionally sampled data are clearly different because they contain an additional focus and two half saddles. The fluctuation levels shown in Figure 10(f) are fairly typical of turbulent jet flow. This is expected because, conditional sampling partly filters out fluctuations due to large-scale jet oscillation, but does not filter out turbulence fluctuations.

Conclusions

The authors have designed and tested an event detector to perform real-time conditional sampling of laser-image data in bi-directional unsteady flows which are not produced by the motion of a mechanical device. The event detector is a mixed analogue-TTL circuit and has three analogue inputs. When the analogue inputs indicate an event arriving from the preferred direction, the detector allows trigger signals to reach the imaging camera.

The event detector has been used for conditionally-sampled PIV in a chamber which produces oscillating jet flow. Streamlines of the conditionally-averaged flow have a spiral focus and two half saddles which are not resolved by simple time averaging.

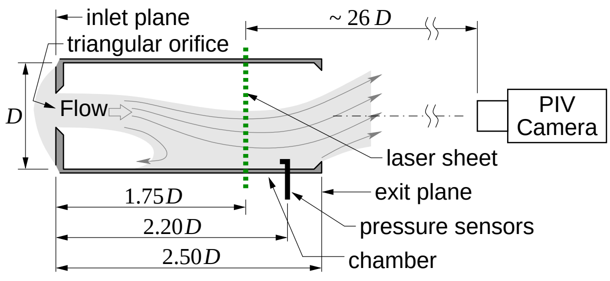

Figure 9: Arrangement for PIV measurements; azimuthal separation between pressure sensors is 30°.

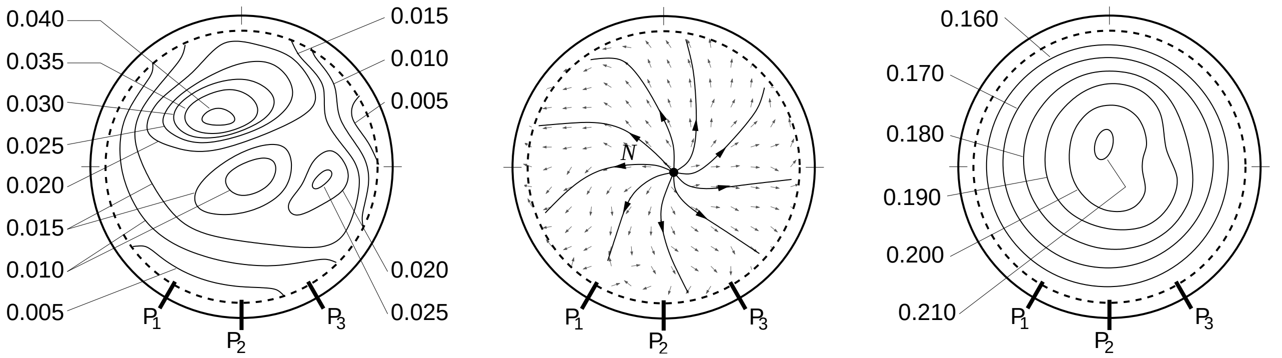

(a) Magnitude of the **un**conditional average, $\sqrt{V^2+W^2}/U_1$.

(b) Streamlines and direction of the **un**conditionally averaged flow;

(c) Magnitude of the **un**conditional r.m.s. fluctuations, $\sqrt{v'^2+w'^2}/U_1$.

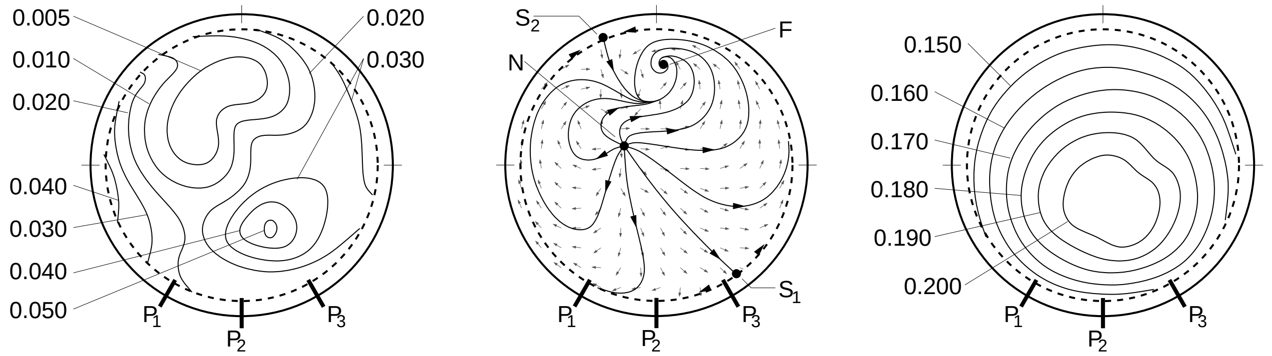

(d) Magnitude of the conditional average, $\sqrt{\langle V\rangle^2+\langle W\rangle^2}/U_1$.

(e) Streamlines and direction of the conditionally averaged flow;

(f) Magnitude of the conditional r.m.s. fluctuations, $\sqrt{\langle v\rangle'^2+\langle w\rangle'^2}/U_1$;

Figure 10: Averaged non-axial $(V\mathbf{i}+W\mathbf{j})$ component of non-dimensional velocity; (a), (b), (c) — unconditionally sampled data; (d), (e), (d) — conditional sampled data; U_1 is mean flow speed at the inlet orifice; only 1 in every 16 of the direction vectors is plotted.

Acknowledgements

The authors offer their thanks to Silvio De Ieso, Derek Franklin and Joel Walker for advice on electronics and for etching the printed circuit, to George Osborne for the pressure sensors, and also to Peter Kalt for setting up and nursing the PIV optics.

References

[1] Antonia, R. A., Conditional sampling in turbulence measurement, *Annu. Rev. Fluid Mech.*, **13**, 1981, 131–156.

[2] Blackwelder, R., On the role of phase information in conditional sampling, *Phys. Fluids*, **20**, 1977, S232–S242.

[3] Guezennec, Y. G., Piomelli, U. and Kim, J., On the shape and dynamics of wall structures in turbulent channel flow, *Phys. Fluids A*, **1**, 1989, 764–767.

[4] Lee, S. K., Lanspeary, P. V., Nathan, G. J., Kelso, R. M. and Mi, J., Low kinetic-energy loss oscillating-triangular-jet nozzles, *Exp. Therm. Fluid Sci.*, **27**, 2003, 553–561.

[5] Li, Y., Zhao, H., Peng, Z. and Ladommatos, N., Particle image velocimetry measurement of in-cylinder flow in internal combustion engines - experiment and flow structure analysis, *P. I. Mech. Eng. D – J. Aut.*, **216**, 2002, 65–81.

[6] Marshall, B. J., Marwood, R., Belcher, R. E. and Wood, C. J., Laser doppler anemometry and conditional sampling, *J. Wind. Eng. Ind. Aerod.*, **79**, 1999, 209–231.

[7] National Semiconductor Corporation, Santa Clara, California, U.S.A., *LM111/LM211/LM311 voltage comparator, datasheet*, 2001.

[8] Subramanian, C. S., Rajagopalan, S., Antonia, R. A. and Chambers, A. J., Comparison of conditional sampling and averaging techniques in a turbulent boundary layer, *J. Fluid Mech.*, **123**, 1982, 335–362.

[9] Van Atta, C. W., Sampling techniques in turbulence measurements, *Annu. Rev. Fluid Mech.*, **6**, 1974, 75–91.

[10] Wernert, P. and Favier, D., Considerations about the phase-averaging method with application to ELDV and PIV measurements over pitching airfoils, *Exp. Fluids*, **27**, 1999, 473–483.

[11] Wong, C. Y., Lanspeary, P. V., Nathan, G. J., Kelso, R. M. and O'Doherty, T., Phase-averaged velocity in a fluidic precessing jet nozzle and in its near external field, *Exp. Therm. Fluid Sci.*, **27**, 2003, 515–524.

[12] Wong, C. Y., Nathan, G. J. and Kelso, R. M., PIV of the unsteady flow emerging from a fluidic precessing jet nozzle using direction and phase triggers, in *Proceedings of 7th Asian Symposium on Visualisation*, National University of Singapore, Singapore, 2003, 22.1–22.6, 22.1–22.6.